



Breast Imaging Original Research

Quantitative classification of invasive and noninvasive breast cancer using dynamic magnetic resonance imaging of the mammary gland

Yoshiaki Miyazaki¹, Juichiro Shimizu², Yuichiro Kubo³, Nobuyuki Tabata³, Tomohiko Aso¹

¹Department of Radiological Technology, National Cancer Center, Chuo-ku, Tokyo, ²Department of Clinical Radiology, Faculty of Health Science, Hiroshima International University, Higashihiroshima, Hiroshima, ³Department of Radiology, National Hospital Organization Kyushu Cancer Center, Minami-Ku, Fukuoka, Japan.



*Corresponding author:

Yoshiaki Miyazaki,
Department of Radiological
Technology, National Cancer
Center, Chuo-ku, Tokyo,
Japan.

yomiyaza@ncc.go.jp

Received : 01 June 2022

Accepted : 15 July 2022

Published : 05 August 2022

DOI

10.25259/JCIS_56_2022

Quick Response Code:



ABSTRACT

Objectives: Breast cancers are classified as invasive or noninvasive based on histopathological findings. Although time-intensity curve (TIC) analysis using magnetic resonance imaging (MRI) can differentiate benign from malignant disease, its diagnostic ability to quantitatively distinguish between invasive and noninvasive breast cancers has not been determined. In this study, we evaluated the ability of TIC analysis of dynamic MRI data (MRI-TIC) to distinguish between invasive and noninvasive breast cancers.

Material and Methods: We collected and analyzed data for 429 cases of epithelial invasive and noninvasive breast carcinomas. TIC features were extracted in washout areas suggestive of malignancy.

Results: The graph determining the positive diagnosis rate for invasive and noninvasive cases revealed that the cut-off $\theta_{i/mi}$ value was 21.6° (invasive: $\theta_w > 21.6^\circ$, noninvasive: $\theta_w \leq 21.6^\circ$). Tissues were classified as invasive or noninvasive using this cut-off value, and each result was compared with the histopathological diagnosis. Using this method, the accuracy of tissue classification by MRI-TIC was 88.6% (380/429), which was higher than that using ultrasound (73.4%, 315/429).

Conclusion: MRI-TIC is effective for the classification of invasive vs. noninvasive breast cancer.

Keywords: Breast cancer, Invasive ductal carcinoma, Noninvasive ductal carcinoma, Computer-aided diagnosis, Time-intensity curve

INTRODUCTION

Mammography and ultrasonography are the first-line diagnostic imaging methods for breast cancer. Magnetic resonance imaging (MRI) is also an important tool for precise preoperative examination of breast tumors because of its high spatial resolution and ability to evaluate blood flow, provide a qualitative diagnosis, and assess the spread of breast tumors. According to Berg *et al.* MRI detects malignancies with a sensitivity of over 95% (167/177), except in cases of special tumors and microscopic lesions; this detection rate was higher than that of mammography (68%; 120/177) and ultrasound (83%; 147/177).^[1]

The time-intensity curve (TIC) [Figure 1] plots the contrast enhancement effect of dynamic MRI over time and is expected to provide a qualitative diagnosis because it reflects the state of blood flow within the tumor.^[2] The diagnostic ability of the TIC to distinguish benign from malignant tumors has been demonstrated in several previous studies.^[3-10]

Malignant mammary gland tumors are divided into two types: invasive cancer, in which the cancer cells break through the ducts and lobules to invade the surrounding tissues in the breast, and noninvasive cancer, in which the cancer cells grow only in the ducts and lobules.^[11,12]

When cancer cells leave the ducts and lobules of the mammary gland, they may metastasize through the blood and lymphatic vessels, greatly affecting the treatment plan and prognosis for life.

Brennan *et al.* reported^[13] that 25.9% of cases diagnosed as noninvasive breast cancer were misdiagnosed, indicating that invasive breast cancer or other cancers were undetected postoperatively. In addition, Sagara *et al.* reported^[14] that in some “noninvasive cancers,” resection and nonresection revealed characteristics that did not significantly differ in survival rates. In other words, the importance of more accurate differentiation between “invasive” and “noninvasive” cancer as the initial management of breast cancer is extremely higher than in the two reports. However, in MRI, qualitative evaluation of the enhancement effect^[2] is the main method for differentiating between invasive and noninvasive lesions, and quantitative evaluation methods have not yet been established.

Therefore, in this study, to evaluate the ability of TIC analysis of dynamic MRI data (MRI-TIC) to distinguish between invasive and noninvasive breast cancers, we extracted TIC features and performed quantitative, pathology-based classification of invasive/noninvasive cancers. Furthermore, we compared the accuracy of MRI-TIC with ultrasonography, which can evaluate blood flow.^[15]

MATERIAL AND METHODS

Study design

This retrospective study included data for 429 cases of invasive (364 cases) and noninvasive (65 cases) breast cancers

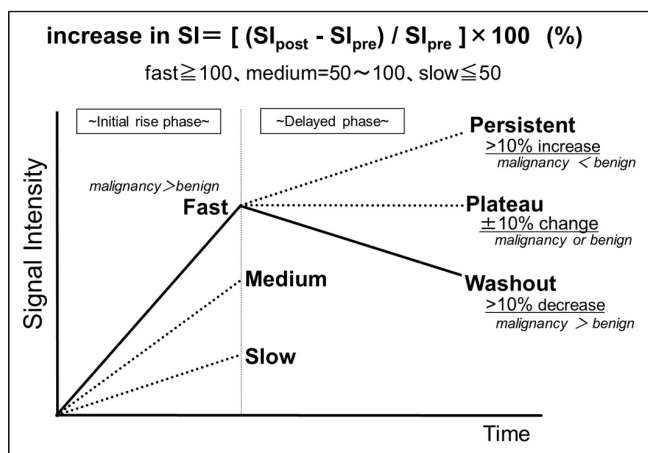


Figure 1: Overview of the time-intensity curve analysis.

diagnosed and treated from April 2016 to March 2018. The inclusion criteria were as follows:^[1] dynamic MRI and ultrasonography were performed,^[2] no chemotherapy was administered, and^[3] a definite diagnosis of invasive or noninvasive cancer was established by pathological examination of the excised lesion.

A 1.5-Tesla MRI device (Siemens Magnetom Symphony; Erlangen, Germany) with a four-channel breast array coil was used to obtain dynamic MRI fat-suppressed T1-weighted images using the gadolinium contrast agent Magnevist IV (Schering Berlin, Germany) and the following parameters: matrix size, 512 × 256; pixel size, 0.6 × 0.8 mm; slice thickness, 1.0 mm; time to repeat, 5.42 s; time to echo, 2.11 s; flip angle, 20°; bandwidth, 300 Hz/pixel, and parallel imaging generalized autocalibrating partial parallel acquisition (GRAPPA; accel. factor PE 2 and ref. lines PE 50). A Sonic Shot GX device (Nemoto Kyorindo Co., Ltd, Tokyo, Japan) was used to inject the contrast medium. The contrast agent (0.2 mL/kg) was injected at a rate of 2.0 mL/s, and 20 mL of physiological saline was boosted at a rate of 2.0 mL/s.

Dynamic MRI was performed using four-time points: before injection of the contrast agent (prephase), immediately after injection of the contrast agent (injection phase), at 60 s (peak phase), and at 300 s (delay phase). The imaging time was 60 s per phase, and there were 96 images taken per phase (384 images total).

All personal information related to the clinical images used in this study was anonymized, except for the MRI, pathological diagnoses, and tumor locations. This study was conducted in accordance with the Declaration of Helsinki. The Ethics Review Committee of the National Hospital Organization Kyushu Cancer Center approved the utilization of data (Approval no. 2016–52) and waived the need for patient consent because of the retrospective nature of the study.

Figure 2 shows the method for distinguishing between invasive and noninvasive breast cancers using MRI-TIC.

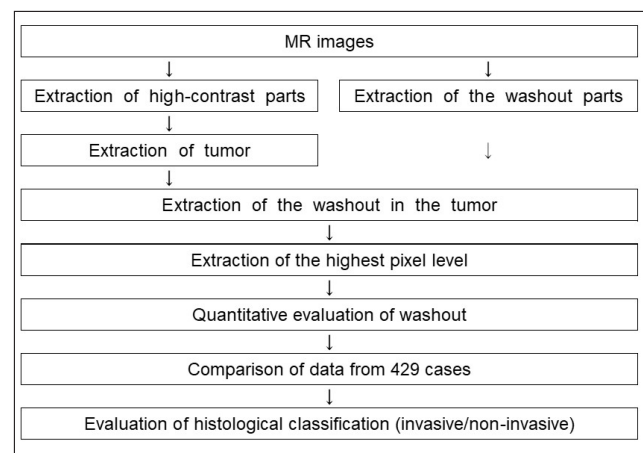


Figure 2: Flowchart for histological classification of invasive/noninvasive cancer.

We investigated the part of the lesion that showed a washout effect, which suggests malignancy. Figure 3 shows the process of extraction of the region with a washout effect in a breast cancer lesion. Automatic extraction was performed as previously reported.^[16]

Invasive/noninvasive classification

Images of lesions with features suggestive of malignancy were automatically extracted from the imaged slices using a 2x2-pixel region of interest (ROI). We defined $\theta_{i/ni}$ as the angle between straight lines A and B in the TIC ($\theta_{i/ni}$) as the angle between straight lines A and B in the TIC (A: a straight line parallel to the time axis and extending from the peak phase, B: a straight line passing through the two points of the peak phase and the delay phase) [Figure 4]. The highest θ value in each case was defined as $\theta_{washout}$ (θ_w), and the classification of invasiveness/noninvasiveness was made according to this value. For all 429 cases, $\theta_{i/ni}$ was calculated as the borderline value of θ_w where the pathological diagnosis was most consistent with the MRI-TIC-based classification by θ_w .

Statistical analysis

All statistical analyses were performed using Excel® 2016 (Microsoft Corporation; Redmond, WA, USA).

Evaluation of the MRI-TIC-based classification by comparison with the postsurgical pathological diagnosis

The sensitivity, specificity, positive predictive value, and negative predictive value for the TIC classification using $\theta_{i/ni}$ were calculated for each histological type (invasive/noninvasive). In addition, accuracy rates for MRI-TIC, and ultrasound results were calculated.

RESULTS

Case details

The patients were women aged 21–88 years (mean 58.2 ± 12.8 years). The tumor diameters were between

0.6 and 9.2 cm (mean 2.1 ± 1.8 cm). Table 1 shows the detailed classification of the target cases according to the World Health Organization (WHO) Classification of Tumors of the Breast.^[11]

Determination of $\theta_{i/ni}$ for distinguishing between invasive and noninvasive lesions

For all 429 cases, the signal intensity in the delay phase was reduced compared to that in the peak phase, and a plateau or washout was observed in MRI-TIC. The graph in Figure 5 shows the θ_w of cases classified as invasive or noninvasive based on the final pathological diagnosis. The θ_w for all cases ranged from 0.7° to 51.8°, with values of 11.2°–51.8° for invasive and 0.7°–32.1° for noninvasive cases. The relationship between the two was $P = 9.7 \times 10^{-52}$.

Figure 6 shows the relationship between the positive diagnosis rate at each θ_w value for cases classified as invasive or noninvasive from pathological diagnoses. For invasive cancer, the positive diagnosis rate showed a gradual decrease from 0° to 20°, after which the slope increased and the positive diagnosis rate decreased. For noninvasive cancer, the positive diagnosis rate reached 52% at 10°, 78% at 20°, and 96% at 30°.

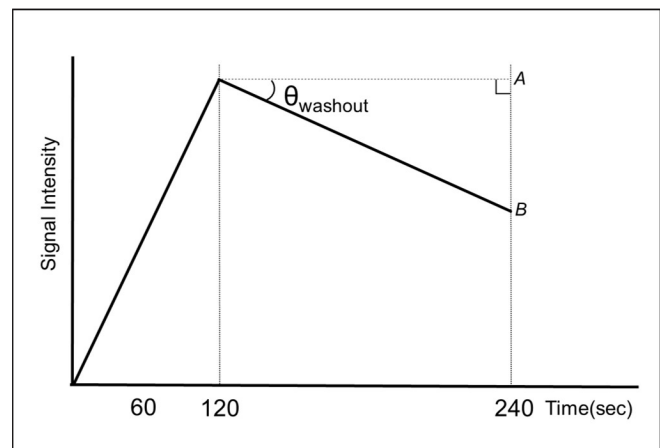


Figure 4: Definition of $\theta_{washout}$ in invasive/noninvasive classification using TIC.



Figure 3: Extraction of the region with a washout effect in breast cancer using images processed by a computer-aided diagnosis program in dynamic magnetic resonance imaging Invasive breast cancer tissue from a 42-year-old woman with a 1.0 cm mass is shown.

Table 1: Detailed classification of eligible cases according to the WHO Classification of Breast Tumors.

Organizational type	Number of cases	% of cases
Invasive breast carcinoma		
Invasive breast carcinoma of no special type	312	73.1
Microinvasive carcinoma	4	0.9
Invasive lobular carcinoma	17	4.0
Tubular carcinoma	1	0.2
Cribriform carcinoma	0	0.0
Mucinous carcinoma	18	4.2
Mucinous cystadenocarcinoma	0	0.0
Invasive micropapillary carcinoma	4	0.9
Carcinoma with apocrine differentiation	6	1.4
Metaplastic carcinoma	2	0.5
Noninvasive lobular neoplasia		
Atypical lobular hyperplasia	0	0.0
Lobular carcinoma <i>in situ</i>	3	0.7
Ductal carcinoma <i>in situ</i>		
Ductal carcinoma <i>in situ</i>	62	14.5
Sum total	429	100.0

WHO Classification of Tumours Editorial Board. Breast tumors (medicine). 5th ed. Lyon: IARC Press; 2019. p.68-138.

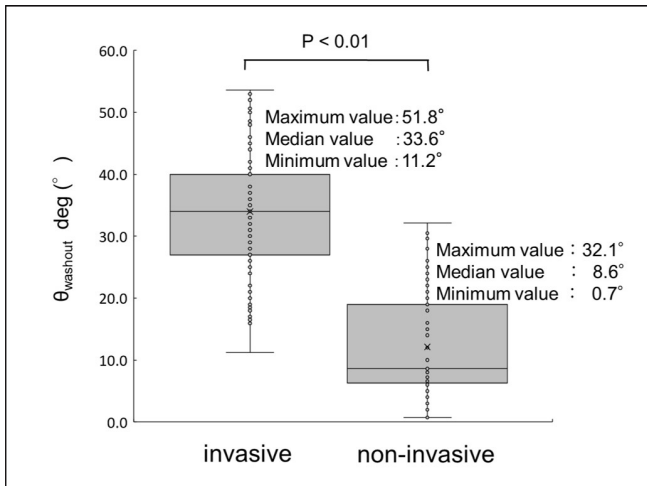


Figure 5: Statistics of $\theta_{washout}$ in pathological diagnosis (invasive/noninvasive).

The graph determining the positive diagnosis rate for invasive and noninvasive cases revealed that the cut-off $\theta_{i/ni}$ value was 21.6° (invasive: $\theta_w > 21.6^\circ$, noninvasive: $\theta_w \leq 21.6^\circ$).

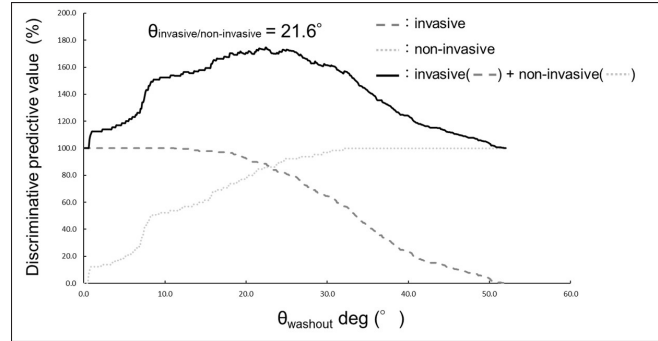


Figure 6: Determination of $\theta_{invasive/noninvasive}$ to classify invasive/noninvasive (Discriminant accuracy in $\theta_{washout}$).

Table 2: Classification of invasive/noninvasive breast carcinoma using time-intensity curve analysis of magnetic resonance imaging data, compared to the diagnosis by pathology ($n = 429$).

Pathological diagnoses	$\theta_{invasive/noninvasive} \leq 21.6^\circ$ (noninvasive)	$\theta_{invasive/noninvasive} > 21.6^\circ$ (invasive)
Invasive breast carcinoma: 364	39/364	325/364
Noninvasive breast carcinoma: 65	55/65	10/65

Effectiveness of MRI-TIC in distinguishing invasive and noninvasive breast carcinoma

Table 2 shows the classification of breast cancer tumors using the $\theta_{i/ni}$ cut-off value of 21.6° for invasiveness/noninvasiveness, which was the most consistent with the pathological diagnoses. The sensitivity, specificity, positive predictive value, and negative predictive value for each tissue are shown in Table 3; these values were 89.3%, 84.6%, 97.0%, and 58.5%, respectively, for invasive tumors and 84.6%, 89.3%, 58.5%, and 97.0%, respectively, for noninvasive tumors. The accuracy of discrimination between invasive and noninvasive cancers using MRI-TIC was 88.6%. Figure 7 shows the classification of invasive ($\theta_{i/ni} > 21.6^\circ$) and noninvasive ($\theta_{i/ni} \leq 21.6^\circ$) breast carcinoma using MRI-TIC and 4-pixel pathological images (size of the ROI, 1.2×1.6 mm).

Comparison of MRI-TIC and ultrasonography

The results of MRI-TIC, and ultrasonography are compared with the pathology results in Table 4. For invasive carcinoma (364 cases), the diagnoses for 325 and 280 cases analyzed by MRI-TIC and ultrasound, respectively, were consistent with the pathological diagnoses. For noninvasive carcinoma (65 cases), the diagnoses for 55 and 35 cases analyzed by MRI-TIC and ultrasound,

Table 3: Effectiveness of time-intensity curve analysis of magnetic resonance imaging data ($\theta_{\text{invasive/noninvasive}}$ cut-off value = 21.6°) in distinguishing invasive and noninvasive breast carcinomas

	Sensitivity	Specificity	Positive predictive value	Negative predictive value	Discriminative predictive value
Invasive breast carcinoma: 364	89.3	84.6	97.0	58.5	88.6
Noninvasive breast carcinoma: 65	84.6	89.3	58.5	97.0	

Values shown are percentages

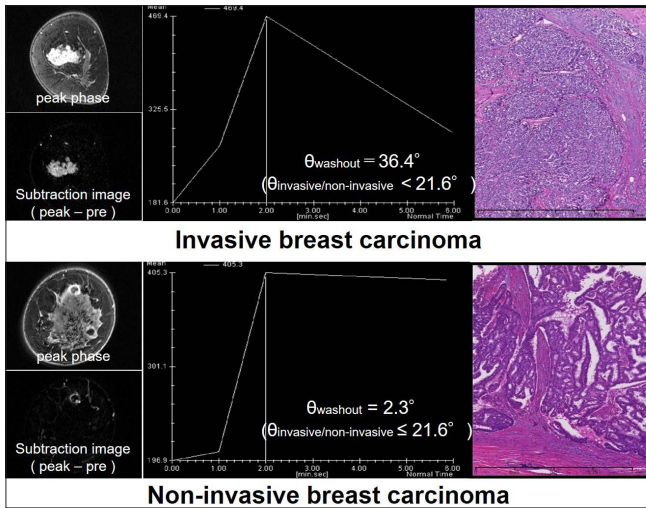


Figure 7: Classification of invasive/noninvasive breast carcinoma using time-intensity curve analysis of magnetic resonance imaging data and pathological images. The size of the region of interest (4 pixels: 1.2×1.6 mm) is the same as the size of the pathology image.

Table 4: Comparison of the results of time-intensity curve analysis of magnetic resonance imaging data and ultrasonography with pathology results for invasive/noninvasive breast carcinoma ($n = 429$)

	MRI-TIC results consistent with pathological diagnosis	Ultrasonography results consistent with pathological diagnosis
Invasive breast carcinoma: 364	325	280
Noninvasive breast carcinoma: 65	55	35
Discriminative predictive value	88.6%	73.4%

TIC: time-intensity curve, MRI: magnetic resonance imaging, Ultrasound results included the first and second differential diagnoses

respectively, were consistent with the pathological diagnoses. The discrimination accuracies of MRI-TIC and ultrasound were 88.6% (380/429) and 73.4% (315/429), respectively, and MRI-TIC was 15.2% (65/429) more accurate than ultrasound in terms of consistency with the pathological diagnosis.

DISCUSSION

In this study, we developed and validated an algorithm for distinguishing between invasive and noninvasive breast cancers using quantitative MRI-TIC for 429 cases. Classification using MRI-TIC was based on $\theta_{i/ni}$, with a cut-off value of 21.6° .

We found that $\theta_{i/ni} > 21.6^\circ$ indicated invasive cancer and $\theta_{i/ni} \leq 21.6^\circ$ indicated noninvasive cancer. They are related by the degree of contrast agent loss after the peak signal intensity, similar to the findings of Kamitani *et al.*^[17] and indicate that the post-peak TIC has a steep trend for invasive cancer and a gradual trend for noninvasive cancer. The difference in $\theta_{i/ni}$ for invasive vs. noninvasive tumors in this study may be the result of differences in histological construction.

In cases of invasive cancer, as the blood concentration of the contrast agent increases, the contrast agent seeps from the blood vessels into the interstitium, resulting in a strong thick stain; this is due to the high vascular density^[18] and increased vascular permeability.^[19] The contrast agent that has leaked into the extravascular interstitium is readily expelled into the vasculature as its blood concentration decreases, and its concentration within the tumor decreases. Because there is little interstitium,^[11,12] the concentration of contrast agent in the tumor tends to decrease quickly and is likely to exhibit a steep washout curve.

In noninvasive cancers, tumor vessels with increased vascular permeability rarely grow.^[19,20] The periductal stroma is wide, and it takes time for the concentration of the contrast agent to increase,^[21] resulting in a poor contrast effect early in the imaging process (slow pattern). The periductal stroma gradually gains contrast, but the contrast agent temporarily pools and drains slowly. Largely because of tumor angiogenesis in the interstitium,^[20] washout is less likely to occur within the examination time, and a plateau or slow washout is seen. In brief, the differences in TIC characteristics are related to the density and permeability of the tumor vessels (noninvasive < invasive) and the size of the stroma (invasive < noninvasive).

Using the pathological diagnoses as a reference, the accuracy of MRI-TIC in distinguishing between invasive and noninvasive breast cancers in this study (364 invasive and 65 noninvasive breast cancers) was 88.6%. Thus, the TIC results did not completely agree with the pathological

diagnoses, possibly because data were collected at only four-time points (prephase, injection phase, peak phase, and delay phase). More time points were not used because the timing technique was not fine-tuned, and this may have caused a discrepancy between the exact peak point and the values at the 2-minute point, which is assumed to be the peak point.^[2] The same can also be said for the washout point; this issue should be investigated further in future research.

Another reason for the lack of complete agreement between MRI-TIC and pathological results was that the invasive/noninvasive tissue classification was determined by observation. It is difficult to observe the entirety of the malignant tissues of a lesion, and judgments based on partial observation may lead to bias among observers and discrepancies in diagnostic results. However, the method of classification of invasive/noninvasive cancers in this study did achieve good quantitative results and compensated for possible subjectivity by scanning all imaging data (396 images: 96 images \times 4 phases) and extracting the washout areas in the tumors. The usefulness of our method is demonstrated by the fact that MRI-TIC-based invasive/noninvasive classifications were consistent with the pathological diagnoses in 88.6% of the 429 cases.

There was a large difference of more than 15.0% in the discrimination accuracy between ultrasound examination, where the first and second differential diagnoses were considered, and our MRI-TIC method. We believe that there are three reasons for this difference. First, ultrasonography findings are affected by the skill of the operator. Second, it is difficult to image the entire lesion. Third, it is difficult to evaluate the lesion quantitatively.

Accurate diagnosis of invasive/noninvasive breast cancer is thought to play a significant role not only in the evaluation of possible metastasis but also in surgical decisions.^[13,14] Since the most accurate information possible from multiple examinations is essential for the diagnosis of breast cancer, this study demonstrates the validity of the quantitative evaluation of invasion/noninvasion in MRI of breast cancer.

We believe that this will help improve pathological diagnosis and will be of great utility in clinical practice.

CONCLUSION

The findings of this study suggest that quantitative MRI-TIC of the mammary glands is effective in distinguishing between invasive and noninvasive breast cancers. We believe that this method can assist physicians in determining the most appropriate treatments for patients with malignant carcinomas.

Declaration of patient consent

Institutional Review Board (IRB) permission obtained for the study.

Financial support and sponsorship

Nil.

Conflict of interest

There are no conflicts of interest.

REFERENCES

1. Berg WA, Gutierrez L, NessAiver MS, Carter WB, Bhargavan M, Lewis RS, *et al.* Diagnostic accuracy of mammography, clinical examination, US, and MR imaging in preoperative assessment of breast cancer. *Radiology* 2004;233:830–49.
2. American College of Radiology. ACR BI-RADS ATLAS breast imaging reporting and data system. In: *Magnetic Resonance Imaging*. 5th ed. United States: American College of Radiology; 2013.
3. Hulka CA, Smith BL, Sgroi DC, Tan L, Edmister WB, Semple JP, *et al.* Benign and malignant breast lesions: Differentiation with echo-planar MR imaging. *Radiology* 1995;197:33–8.
4. Kuhl CK, Mielcareck P, Klaschik S, Leutner C, Wardelmann E, Gieseke J, *et al.* Dynamic breast MR imaging: Are signal intensity time course data useful for differential diagnosis of enhancing lesions? *Radiology* 1999;211:101–10.
5. Jansen SA, Fan X, Karczmar GS, Abe H, Schmidt RA, Newstead GM. Differentiation between benign and malignant breast lesions detected by bilateral dynamic contrast-enhanced MRI: A sensitivity and specificity study. *Magn Reson Med* 2008;59:747–54.
6. Bhooshan N, Giger ML, Jansen SA, Li H, Lan L, Newstead GM. Cancerous breast lesions on dynamic contrast-enhanced MR images: Computerized characterization for image-based prognostic markers. *Radiology* 2010;254:680–90.
7. Jansen SA, Shimauchi A, Zak L, Fan X, Karczmar GS, Newstead GM. The diverse pathology and kinetics of mass, nonmass, and focus enhancement on MR imaging of the breast. *J Magn Reson Imaging* 2011;33:1382–9.
8. Agliozzo S, de Luca M, Bracco C, Vignati A, Giannini V, Martincich L, *et al.* Computer-aided diagnosis for dynamic contrast-enhanced breast MRI of mass-like lesions using a multiparametric model combining a selection of morphological, kinetic, and spatiotemporal features. *Med Phys* 2012;39:1704–15.
9. Mann RM, Mus RD, van Zelst J, Geppert C, Karssemeijer N, Platel B. A novel approach to contrast-enhanced breast magnetic resonance imaging for screening: High-resolution ultrafast dynamic imaging. *Invest Radiol* 2014;49:579–85.

10. Abe H, Mori N, Tsuchiya K, Schacht DV, Pineda FD, Jiang Y, *et al.* Kinetic analysis of benign and malignant breast lesions with ultrafast dynamic contrast-enhanced MRI: Comparison with standard kinetic assessment. *AJR Am J Roentgenol* 2016;207:1159–66.
11. WHO Classification of Tumours Editorial Board. Breast tumours (medicine). 5th ed. Lyon: IARC Press; 2019. p. 102–9.
12. Japanese Breast Cancer Society. General rules for clinical and pathological recording of breast cancer. 18th ed. Tokyo: Kanehara Shuppan; 2018. p. 24–30.
13. Brennan ME, Turner RM, Ciatto S, Marinovich ML, French JR, Macaskill P, *et al.* Ductal carcinoma in situ at core-needle biopsy: Meta-analysis of underestimation and predictors of invasive breast cancer. *Radiology* 2011;260:119–28.
14. Sagara Y, Mallory MA, Wong S, Aydogan F, DeSantis S, Barry WT, *et al.* Survival benefit of breast surgery for low-grade ductal carcinoma in situ: A population-based cohort study. *JAMA Surg* 2015;150:739–45.
15. Iwamoto H, Terashima S, Tanaka K, Karagan T, Hashiyama R, Komiya N, *et al.* Role of ultrasonic flow imaging diagnosis in differential classification of Ductal Carcinoma in situ. *Japanese J Med Ultrasound* 2014;39:449–57.
16. Miyazaki Y, Tabata N, Taroura T, Shinozaki K, Kubo Y, Tokunaga E, *et al.* [Development of a computer-aided diagnosis system to distinguish between benign and malignant mammary tumors in Dynamic magnetic resonance images: Automatic detection of the position with the strongest washout effect in the tumor]. *Nihon Hoshasen Gijutsu Gakkai Zasshi* 2108;74:251–61.
17. Kamitani T, Noguchi T, Saku M. Dynamic MR mammography. Differences of time-intensity curve among each histology. *Jpn J Breast Cancer* 2003;18:240–5.
18. Furuta A, Ishibashi T, Takahashi S, Yamada S, Ohuchi N, Amano G, *et al.* Magnetic resonance imaging of breast cancer: Correlation between contrast enhancement and tumor angiogenesis. *Nippon Acta Radiol* 1999;59:682–8.
19. García-Román J, Zentella-Dehesa A. Vascular permeability changes involved in tumor metastasis. *Cancer Lett* 2013;335: 259–69.
20. Li R, Zheng K, Yuan C, Chen Z, Huang M. Be active or not: The relative contribution of active and passive tumor targeting of nanomaterials. *Nanotheranostics* 1:346–357.
21. Gilles R, Zafrani B, Guinebretière JM, Meunier M, Lucidarme O, Tardivon AA, *et al.* Ductal carcinoma in situ: MR imaging-histopathologic correlation. *Radiology* 1995;196:415–9.

How to cite this article: Miyazaki Y, Shimizu J, Kubo Y, Tabata N, Aso T. Quantitative classification of invasive and noninvasive breast cancer using dynamic magnetic resonance imaging of the mammary gland. *J Clin Imaging Sci* 2022;12:45.